

Multicanonical Ensemble Generated by Molecular Dynamics Simulation for Enhanced Conformational Sampling of Peptides

Nobuyuki Nakajima,[†] Haruki Nakamura,[‡] and Akinori Kidera*

Biomolecular Engineering Research Institute, 6-2-3 Furuedai, Suita, Osaka 565, Japan

Received: July 16, 1996; In Final Form: September 17, 1996[⊗]

A molecular dynamics (MD) method using the multicanonical algorithm, multicanonical MD, is proposed to enhance the efficiency of conformational sampling of peptides. Multicanonical MD is a constant temperature MD on a deformed potential energy surface, which gives a multicanonical ensemble characterized by a flat energy distribution. The multicanonical ensemble, in turn, is converted into a canonical ensemble by the reweighting formula of Ferrenberg and Swendsen. The multicanonical algorithm was originally developed by Berg et al. as a method of Monte Carlo simulations. The multicanonical MD is its application to MD simulations. Using a system of a simple double-well potential, it was confirmed that this method yields a correct canonical distribution. A test of the method was also performed with a five-residue peptide, Met-enkephalin, and showed that multicanonical MD samples much larger conformational space than conventional canonical MD.

1. Introduction

Understanding the mechanisms of protein folding and molecular recognition is one of the most important objectives of structural biology. In these biological processes, proteins cross over vast areas of the conformational space to change their structures. Conformational sampling by Monte Carlo (MC) or molecular dynamics (MD) simulations has been used to study such structural changes or fluctuations. Even though these computer simulation techniques have played important roles in structural biology, the sampling efficiencies are far from satisfactory. In the traditional simulation methods, the trajectories tend to get trapped at local minima close to the starting coordinates, due to the energy barriers surrounding the low energy regions.

Recently, a new method of MC simulation, called the multicanonical algorithm, has been proposed by Berg et al.^{1–3} and has been used to improve the sampling efficiency in a variety of systems,^{4–9} including peptides and proteins.^{10–13} The algorithm affords an extremely high sampling efficiency by artificially flattening the energy spectra and yields a “multicanonical ensemble”. Then this ensemble is transformed into a canonical ensemble at an arbitrary temperature by the reweighting formula of Ferrenberg and Swendsen.¹⁴

The algorithm of the multicanonical MC method is briefly reviewed here.^{1,4,13} In the canonical ensemble at a temperature T , the probability distribution function, P_c , of the potential energy E is given by

$$P_c(E, T) = \left(\frac{1}{Z_c} \right) n(E) e^{-E/kT} \quad (1)$$

where $n(E)$ is the spectral density and $Z_c = \sum_E n(E) e^{-E/kT}$. When P_c is plotted against E , it shows a Gaussian-like distribution peaked around the ensemble average $\langle E \rangle$. In this form of the

function, at a lower temperature T , there is a very small probability of overcoming the energy barriers because of the small value of P_c in the high-energy region. At a higher temperature T , on the other hand, P_c is so small in the low-energy region that it is difficult to obtain the precise distribution at room temperature. Such a problem can be solved by a multicanonical ensemble, which is characterized by the following artificial flat energy distribution, P_{mc} :

$$P_{mc}(E) = \frac{1}{Z_{mc}} n(E) e^{-W(E)} = \text{constant} \quad (2)$$

where $W(E)$ is a function of E , and $Z_{mc} = \sum_E n(E) e^{-W(E)}$. This flat energy distribution brings about a high probability of surmounting the energy barriers and a high probability of sampling the low energy regions. For a given $W(E)$ satisfying eq 2, a multicanonical MC simulation can be carried out with the Metropolis criterion $\min(1, \exp[-W(E_n) + W(E_m)])$.¹⁵ After the simulation, the reweighting formula derived from eqs 1 and 2 converts P_{mc} into the canonical distribution, P_c , at an arbitrary temperature T as¹⁴

$$P_c(E, T) = \frac{1}{Z_c} n(E) e^{-E/kT} = \frac{Z_{mc}}{Z_c} P_{mc}(E) e^{W(E) - E/kT} \quad (3)$$

In practice, the function $W(E)$ is not given *a priori*, but is determined from a preliminary canonical simulation at a sufficiently high temperature T_0 as,

$$W(E) = \ln n(E) = (E/kT_0) + \ln P_c(E, T_0) \quad (4)$$

where the energy-independent terms are neglected. When $P_c(E, T_0)$ does not cover a sufficiently large E range, the weight function $W(E)$ can be refined iteratively in several multicanonical MC runs by using the following relation derived from eq 2:

$$W^{i+1}(E) = W^i(E) + \ln P_{mc}^i(E) \quad (5)$$

where the i th multicanonical distribution $P_{mc}^i(E)$ is obtained with the weight function $W^i(E)$.

[†] E-mail: nakajima@beri.co.jp.

[‡] E-mail: nakamura@beri.co.jp.

* To whom all correspondence should be addressed. E-mail: kidera@qchem.kuchem.kyoto-u.ac.jp. Present address: Graduate School of Science, Kyoto University, Kitashirakawa, Sakyo-ku, Kyoto 606-01, Japan.

[⊗] Abstract published in *Advance ACS Abstracts*, January 1, 1997.

For the chain molecules such as proteins, MC simulations have been carried out mostly in the dihedral angle space, not in the Cartesian space. In the Cartesian space, it is difficult to form a trial MC step in such a way as to maintain the covalent geometry of a chain molecule.¹⁶ In the dihedral angle space, on the other hand, the covalent geometry is always maintained. However, there is a drawback in the MC simulation of the dihedral angle space. When a system contains many molecules, such as a protein molecule bound with substrates and surrounded by solvent molecules, the system possesses both internal and external degrees of freedom. The coexistence of two kinds of variables makes the simulation algorithm very complex. In such a case, simulations in the Cartesian space, containing only external variables, are preferable.

To avoid these problems in the MC simulation, we have applied the multicanonical algorithm to the MD simulation in the Cartesian space. In this paper, we propose a method for such an MD simulation, multicanonical MD. By means of this method, we can efficiently obtain the multicanonical ensemble for a system of chain molecules.

First, we will describe the algorithm of multicanonical MD. Second, it is shown that the multicanonical MD of a model system with a double-well potential correctly gives the canonical ensemble. Finally, from the application of multicanonical MD to a five-residue peptide, Met-enkephalin, we will show that multicanonical MD is a much more efficient method of conformational sampling than conventional canonical MD.

2. Theory and Methods

2.1. Formulation of Multicanonical MD. Here we describe the application of the multicanonical algorithm to MD simulations. The goal is to generate the multicanonical ensemble, defined in eq 2, by integrating the Newtonian equation. In multicanonical MC, the Boltzmann factor, $\exp(-E/kT)$, has been modified to the function $\exp[-W(E)]$, to obtain the multicanonical ensemble. In MD simulations, because both the potential energy E and the kinetic energy, or the temperature T , have to be given explicitly, E and T of the multicanonical ensemble, E_{mc} and T_{mc} , respectively, should be given as a function of the internal energy E . For the sake of simplicity, we consider the following two cases. In the first case, the temperature $T_{mc}(E)$ is fixed at the same temperature as that of the preliminary canonical simulation, i.e., $T_{mc}(E) = T_0$, and the potential energy $E_{mc}(E)$ is scaled so as to satisfy eq 2. The second case is given by making the potential energy $E_{mc}(E)$ the same as that of the canonical simulation, i.e., $E_{mc}(E) = E$, and by scaling the temperature $T_{mc}(E)$. We call the former the potential scaling method, and the latter the temperature scaling method.

The potential scaling method generates an artificial ensemble with a deformed potential energy $E_{mc}(E)$ at a constant temperature T_0 . This can be regarded as the canonical ensemble with the potential energy E_{mc} . Therefore, the deformed potential energy $E_{mc}(E)$ is defined from eqs 1 and 2 by

$$W(E) = E_{mc}(E)/kT_0 \quad (6)$$

and thus

$$E_{mc}(E) = E + kT_0 \ln P_c(E, T_0) \quad (7)$$

This method can be considered as a type of umbrella sampling,^{17–19} with the umbrella potential $E_{mc}(E) - E$.

In the temperature scaling method, on the other hand, we have to consider an artificial ensemble at the energy-dependent temperature $T_{mc}(E)$. According to Berg et al.,^{1,20} $T_{mc}(E)$ is

defined as a microcanonical temperature by

$$\frac{1}{T_{mc}(E)} = k \frac{\partial \ln n(E)}{\partial E} = \frac{1}{T_0} + k \frac{\partial \ln P_c(E, T_0)}{\partial E} \quad (8)$$

Berg et al. adopted eq 8 in defining the weight function $W(E)$ for the multicanonical MC simulation as

$$W(E) = \beta(E)E + \alpha(E) \quad (9)$$

where

$$\alpha(E) = \ln P_c(E, T_0) - E \frac{\partial \ln P_c(E, T_0)}{\partial E} \quad (10)$$

$$\beta(E) = 1/kT_{mc}(E) \quad (11)$$

It is noted that both forms of the weight functions, eqs 6 and 9, are derived from the same equation, eq 4, and therefore give the same results in the multicanonical MC simulations. However, in the multicanonical MD simulations, these two methods are totally different, because they are equivalent in the configuration space, whereas they are very different in the momentum space.

The difference between the potential scaling and the temperature scaling methods can be found in their generalized Liouville equations. In conventional MD simulations at a constant temperature T_0 , the time derivative of the probability distribution P_c is derived from the generalized Liouville equation:

$$\frac{dP_c}{dt} = -\frac{1}{kT_0} \frac{dH}{dt} P_c \quad (12)$$

where

$$H = K + E \quad \text{for the constraint method,}^{21} \text{ or} \quad (13)$$

$$H = K + E + K^R \quad \text{for the Nosé–Hoover method}^{22} \quad (14)$$

Here K is the kinetic energy of the system, and K^R is that of the heat reservoir. The solution of eq 12 is simply

$$P_c \propto e^{-H/kT_0} \quad (15)$$

This equation guarantees that these two methods of the constant temperature MD simulations give the canonical distribution.²³ Particularly, in the constraint method (eq 13), the kinetic energy is constant, $dK/dt = 0$, and thus eq 15 is rewritten by

$$P_c \propto e^{-E/kT_0} \quad (16)$$

Since the potential scaling multicanonical MD can be considered simply as a constant temperature MD simulation on the deformed potential energy surface E_{mc} , the same form of equation as eq 12 holds in the time derivative of the probability distribution P_{mc} , i.e.

$$\frac{dP_{mc}}{dt} = -\frac{1}{kT_0} \frac{dE_{mc}}{dt} P_{mc} \quad (17)$$

where only the E -dependent term is retained. Using the definition of the weight function $W(E)$, eq 6, we have the solution of eq 17 as

$$P_{mc} \propto e^{-E_{mc}/kT_0} = e^{-W(E)} \quad (18)$$

This means that P_{mc} is the canonical distribution of E_{mc} . From eq 18, we recover the basic equation for the multicanonical ensemble, eq 2:

$$P_{mc}(E) = \left(\frac{1}{Z_{mc}}\right)n(E)e^{-W(E)} = \text{constant} \quad (19)$$

This proves that the potential scaling multicanonical MD by either the constraint method or the Nosé–Hoover method correctly yields the multicanonical ensemble that satisfies eq 2.

On the other hand, in the temperature scaling multicanonical MD, we consider controlling the temperature $T_{mc}(E)$ by using either of the two methods above. In this case, the time derivative of the multicanonical distribution P_{mc} becomes

$$\frac{dP_{mc}}{dt} = -\frac{1}{kT_{mc}(E)} \frac{dH_{mc}}{dt} P_{mc} \quad (20)$$

where

$$H_{mc} = K_{mc}(E) + E \quad \text{for the constraint method, or} \quad (21)$$

$$H_{mc} = K_{mc}(E) + E + K_{mc}^R(E) \quad \text{for the Nosé–Hoover method} \quad (22)$$

Here, the kinetic energies of the system and the reservoir, K_{mc} and K_{mc}^R , are both functions of E , or time t , because T_{mc} defined in eq 8 is dependent on E (or time). In the constraint method (eq 21), K_{mc} is simply equal to $1/2 N k T_{mc}$ (N being the number of degrees of freedom), and the solution of eq 20 becomes

$$P_{mc} \propto e^{-W(E) - 1/2 N \ln T_{mc}} \quad (23)$$

This solution has an additional term, $\exp(-1/2 N \ln T_{mc})$, as compared to the definition of the multicanonical ensemble, eq 2. In the Nosé–Hoover method (eq 22), the complicated time dependence of K_{mc} and K_{mc}^R does not allow us to solve eq 20 analytically, but at any rate, the probability distribution P_{mc} should be different from eq 2. Hence, as long as the scaled temperature $T_{mc}(E)$ defined in eq 8 is controlled, by using either the constraint method or the Nosé–Hoover method, the temperature scaling multicanonical MD does not generate the multicanonical ensemble. In the following simulations of multicanonical MD, we used the potential scaling method, and not the temperature scaling method.

2.2. Computations. **2.2.1. Equations of Motion.** As a thermostat in the multicanonical MD, we have adopted the constraint method in which the total kinetic energy is constant.^{24,25} The reason why we chose the constraint method, not the Nosé–Hoover method, is explained in the Results and Discussion.

The equations of motion of the constraint method are given by

$$\dot{\mathbf{q}}_i = \frac{d\mathbf{q}_i}{dt} = \frac{\mathbf{p}_i}{m_i} \quad (24)$$

$$\dot{\mathbf{p}}_i = \mathbf{f}_i^{mc} - \xi \mathbf{p}_i \quad (25)$$

where m_i , \mathbf{q}_i , and \mathbf{p}_i are the mass, coordinate, and momentum for atom i . The force \mathbf{f}_i^{mc} acting on atom i is calculated from $E_{mc}(E)$ (eq 7) by

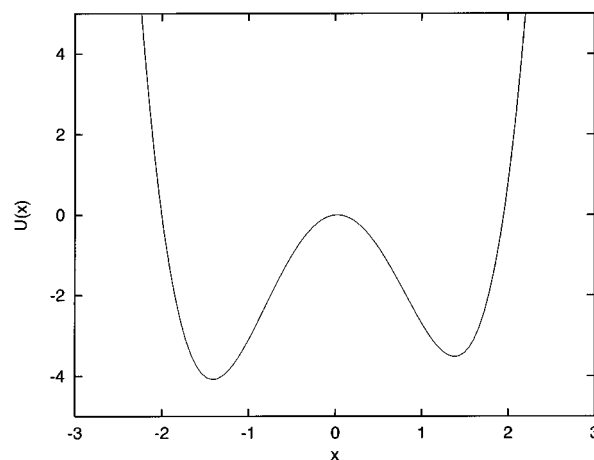


Figure 1. Potential energy function $U(x)$ of the model system, given by eq 28.

$$\mathbf{f}_i^{mc} = -\frac{\partial E_{mc}}{\partial \mathbf{q}_i} = -\frac{dE_{mc}}{dE} \frac{\partial E}{\partial \mathbf{q}_i} \quad (26)$$

The coefficient ξ is chosen so as to guarantee that the total kinetic energy is constant:

$$\xi = \frac{\sum_i \mathbf{f}_i^{mc} \cdot \dot{\mathbf{q}}_i}{2 \sum_i \mathbf{p}_i^2 / 2m_i} = -\frac{dE_{mc}/dt}{NkT_0} \quad (27)$$

where N is the number of degrees of freedom and T_0 is the constant temperature. We integrate these equations by the leapfrog method.^{26,27}

2.2.2. Model System with a Double-Well Potential. For a verification of the current method, we first considered a model system of 48 noninteracting particles, assuming that all of the physical quantities, such as energy and time, are properly converted into dimensionless variables. The potential energy function is that of a one-dimensional double well (Figure 1) given by

$$U(x) = [(x+1)^2 - 1][(x-1)^2 - 0.9] \quad (28)$$

This double well potential is simple enough to give the analytical form of the canonical distribution at a temperature T :

$$P(x) = C e^{-U(x)/kT} \quad (29)$$

where C is the normalization constant. Moreover, it is not as stiff as a simple harmonic potential, in which MD simulations encounter the problem of nonergodicity and do not provide the correct canonical distribution.^{22,28}

The potential energy function $E_{mc}(E)$ for the multicanonical MD was determined by the following procedure, which is similar to that used in the multicanonical MC.¹³ First, a preliminary canonical MD simulation was carried out at a sufficiently high temperature, $kT_0 = 2$, to overcome the energy barriers. Second, the resultant probability distribution $P_c(E, T_0)$, with a bin size of 0.5, was fitted and extrapolated by a polynomial function. To avoid oversampling the very-high-energy conformations, we connected the polynomial smoothly to a linear function for the region of $E \geq -125$. Finally, the deformed potential function $E_{mc}(E)$ was determined by eq 7 with the extrapolated canonical distribution $P_c(E, T_0)$. We carried out a multicanonical MD simulation at $kT_0 = 2$. In both of the

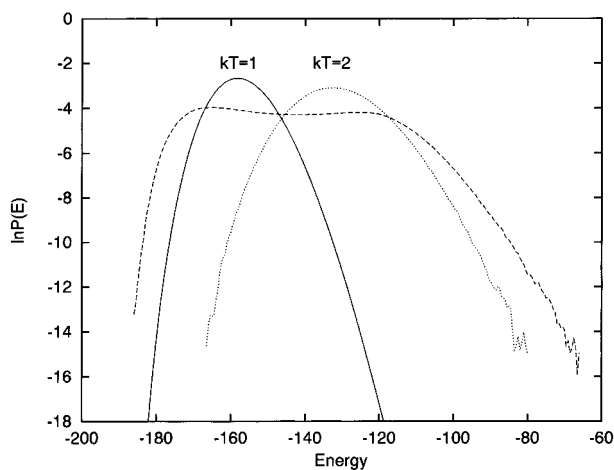


Figure 2. Energy distributions of the model system with the double-well potential (Figure 1). The dotted curve is that of the preliminary canonical MD at $kT = 2$. The broken curve is that of the multicanonical MD at $kT = 2$. The solid curve is the distribution at $kT = 1$ obtained by the reweighting formula (eq 3).

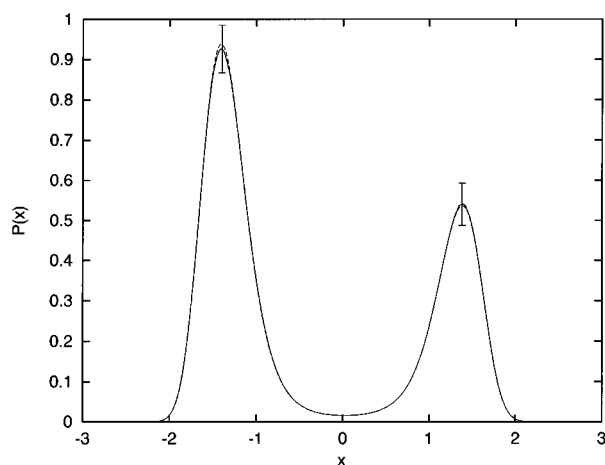


Figure 3. Probability distributions of the coordinate x at $kT = 1$ for the model system with the double-well potential (Figure 1). The solid curve is the average of the distributions at $kT = 1$ for the 48 particles, which are calculated by reweighting the results of the multicanonical MD. The error bars are the standard deviations at the two maxima. The broken curve is the analytical distribution function $P(x)$, given by eq 29.

simulations, the following conditions were adopted: the time step for the leapfrog method is 0.002, the number of steps for each run is 1×10^8 , the mass of a particle is 1.0, and the initial coordinates and the initial velocities were determined randomly. The resultant multicanonical distribution $P_{mc}(E)$ was reweighted by eq 3 to obtain the distribution functions $P_i(x)$ ($i = 1, 2, \dots, 48$) for each particle at $kT = 1$.

2.2.3. Met-enkephalin. The second system for a test of the algorithm is a five-residue peptide, Met-enkephalin (Tyr-Gly-Gly-Phe-Met). No solvent molecules are included in the simulation. Its N- and C-termini are capped with an acetyl and an N-methyl group, respectively, to avoid artifacts in the simulation in vacuo. MD simulations were performed by the program PRESTO²⁹ with a minor modification for the multicanonical MD. The force field parameters are those of the all atom version of AMBER.³⁰ The time step (Δt) is 0.5 fs, and the initial coordinates are those of a fully extended structure with the torsion angles of the main chain, ϕ , ψ , and ω , at 180° .

In the same way as the model system, the potential energy function $E_{mc}(E)$ for the multicanonical MD was determined in the following manner, which is similar to that used in the

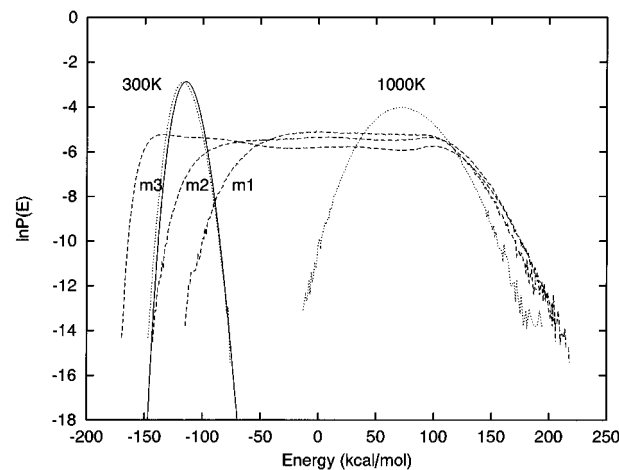


Figure 4. Energy distributions of Met-enkephalin. The dotted curves represent the results of the canonical MD at 300 and 1000 K. The broken curves show the results of the multicanonical MD. The curves m1, m2, and m3 are the distributions, $P_{mc}^i(E)$ ($i = 1, 2, 3$), of the first, second, and third multicanonical MD, respectively, performed on the potential energy $E_{mc}(E)$, refined by eq 5.

multicanonical MC.¹³ First, a preliminary canonical MD was carried out for 2×10^6 steps at a sufficiently high temperature, $T_0 = 1000$ K. Second, the resultant probability distribution $P_c(E, T_0)$, with a bin size of 1.0 kcal/mol, was fitted and extrapolated by a polynomial function. The polynomial function was smoothly connected to a linear function for the region of $E \geq -90$ kcal/mol. Finally, the deformed potential function $E_{mc}(E)$ was determined by eq 7. A multicanonical MD simulation was carried out for 1×10^6 steps at $T_0 = 1000$ K. To sample the low-energy conformations sufficiently, we iterated these processes twice to refine the potential energy $E_{mc}(E)$, by using eq 5. During this iteration, we increased the simulation steps up to 2×10^6 and 1×10^7 for the second and third multicanonical MD runs, respectively. After the third simulation, we calculated the canonical distribution at $T = 300$ K by the reweighting formula (eq 3). As a reference, we performed a canonical MD simulation at $T = 300$ K separately, under the same conditions as the third multicanonical simulation run. All simulations were carried out on a DEC Alpha Station 600 5/266.

3. Results and Discussion

3.1. Model System with a Double-Well Potential. Figure 2 shows the energy distributions of the model system with a double-well potential, the multicanonical distribution (broken curve), and two of the canonical distributions, at $kT = 2$ (dotted curve) and at $kT = 1$ (solid curve). The canonical distribution at $kT = 1$ was obtained by the reweighting formula (eq 3) from the multicanonical distribution. The multicanonical distribution is flat enough to cover a wide range of the conformational energy. In the same way as the energy distribution, the canonical distribution along the one-dimensional variable x , $P(x)$, can be calculated by reweighting the multicanonical distribution. Figure 3 shows a comparison of the simulation result in the form of the average for the 48 particles (solid curve) with the analytical solution of eq 29 (broken curve). They show good agreement. Therefore, it is concluded that we obtained the correct canonical distribution by reweighting the result of the multicanonical MD, as expected in the solution of the generalized Liouville equation, eq 18.

3.2. Met-enkephalin. Figure 4 shows the energy distributions of Met-enkephalin in vacuo. It emphasizes how the iteration procedure enhances the range of the energy distribution.

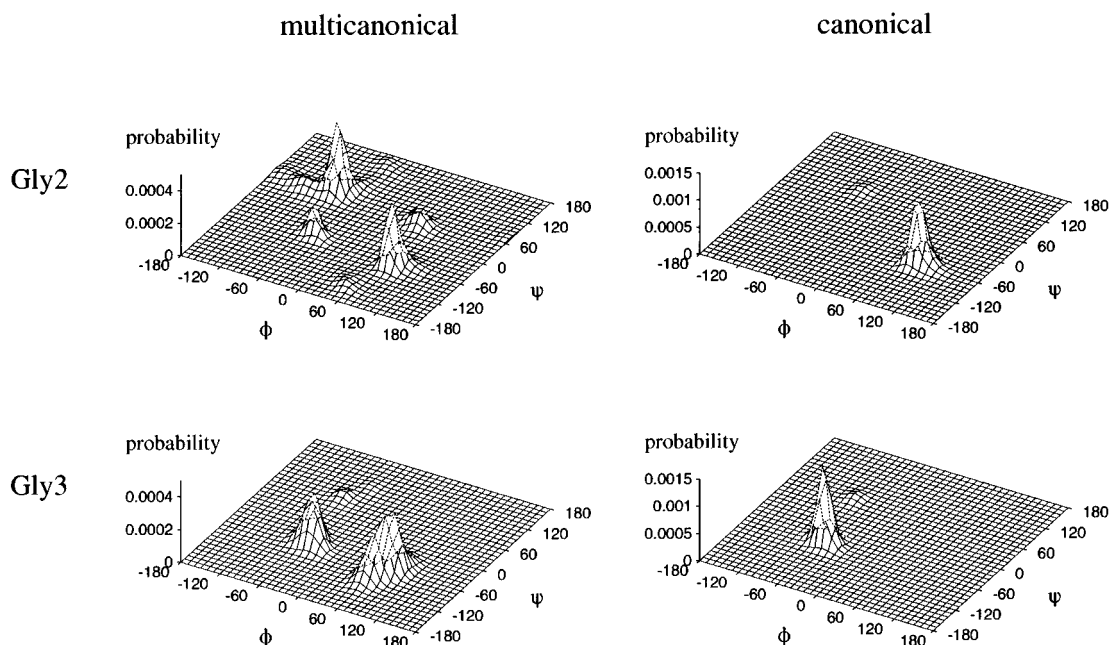


Figure 5. Conformational distributions of the torsion angles, ϕ and ψ , of Gly2 and Gly3 of Met-enkephalin. The figures on the left (indicated as multicanonical) are the canonical distribution at 300 K obtained by reweighting the results of the multicanonical MD. The figures on the right (indicated as canonical) are those of the results of the canonical MD at 300 K.

After two iteration procedures to refine the function $E_{mc}(E)$, we obtained a flat energy distribution covering a wide range of the conformational energy. The canonical distribution at 300 K calculated from the multicanonical distribution (solid curve) seems to be very similar to that of the canonical MD at 300 K (dotted curve). Therefore, as far as the energy distributions are concerned, there are no distinct differences between the multicanonical and the canonical MD simulations.

However, the two methods generated significantly different results in the conformational distribution. In Figure 5, the distributions at 300 K are plotted in terms of the torsion angles, ϕ and ψ , of Gly2 and Gly3 of Met-enkephalin. The figures on the left (indicated as multicanonical) are the canonical distribution at 300 K obtained by reweighting the results of the multicanonical MD. The figures on the right (indicated as canonical) are the results of the canonical MD at 300 K. The difference between these two sets of figures indicates that the canonical MD simulation is confined in much smaller conformational space than that of the multicanonical MD.

A different representation of the conformational distribution is given in Figure 6. The main chain conformations of Gly2 and Gly3 are classified into 16 groups in terms of the torsion angles, ϕ_2 , ψ_2 , ϕ_3 , and ψ_3 . Each group is defined by whether each torsion angle is positive or negative. Combining the results shown in Figures 5 and 6, we find that the canonical MD simulation at 300 K sampled mostly only one conformation [$(\phi_2, \psi_2, \phi_3, \psi_3) \cong (90^\circ, -60^\circ, -60^\circ, -60^\circ)$]. On the other hand, the reweighted distribution of the multicanonical MD indicates that there are two major conformations; one is the same as that of the canonical MD, the other is a completely different conformation [$(\phi_2, \psi_2, \phi_3, \psi_3) \cong (-80^\circ, 60^\circ, 80^\circ, -60^\circ)$]. The probability of the latter conformation is higher than that of the former, and the latter becomes more dominant than the former when the temperature decreases from 300 K (filled bar) to 200 K (white bar). These distributions are consistent with the result of the energy minimization³¹ using ECEPP/2 force field parameters,³² where the torsion angles of the minimum-energy conformation are $(\phi_2, \psi_2, \phi_3, \psi_3) = (-154^\circ, 83^\circ, 84^\circ, -74^\circ)$. The highest probability conformation in the multicanonical MD is close to this minimum-energy conformation. The differences

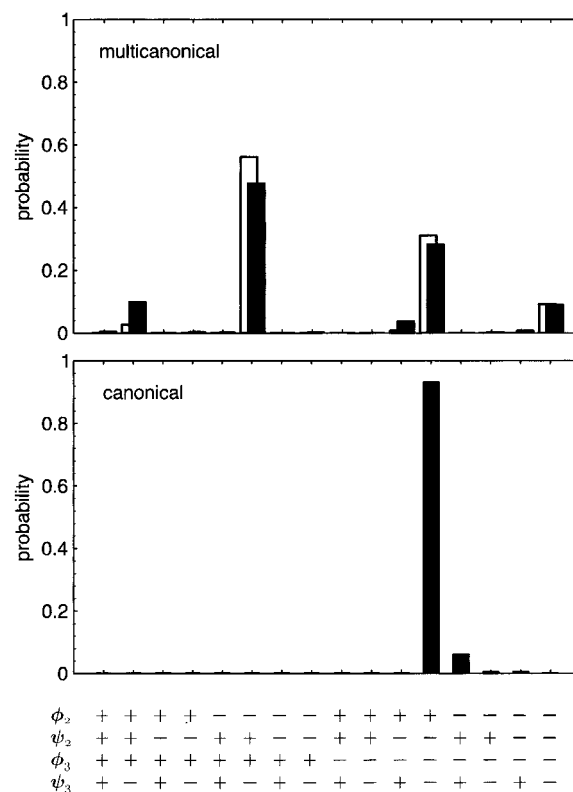


Figure 6. Frequency distributions for 16 groups classified by the signs of the four torsion angles, ϕ_2 , ψ_2 , ϕ_3 , and ψ_3 , which are ϕ and ψ of Gly2 and ϕ and ψ of Gly3, respectively ($-180^\circ \leq \phi_2, \psi_2, \phi_3, \psi_3 \leq 180^\circ$). The upper histogram shows both of the canonical distributions at 300 K (filled bar) and at 200 K (white bar) obtained by reweighting the results of the multicanonical MD. The lower histogram is the distribution at 300 K obtained by the canonical MD.

in the torsion angles may be due to the differences in the force field parameters between AMBER and ECEPP/2, and in the influence of the end groups in this system. Therefore, it is understood that the trajectories of the canonical MD at 300 K were trapped in the high-energy regions close to the initial coordinates but were far from the minimum-energy structure.

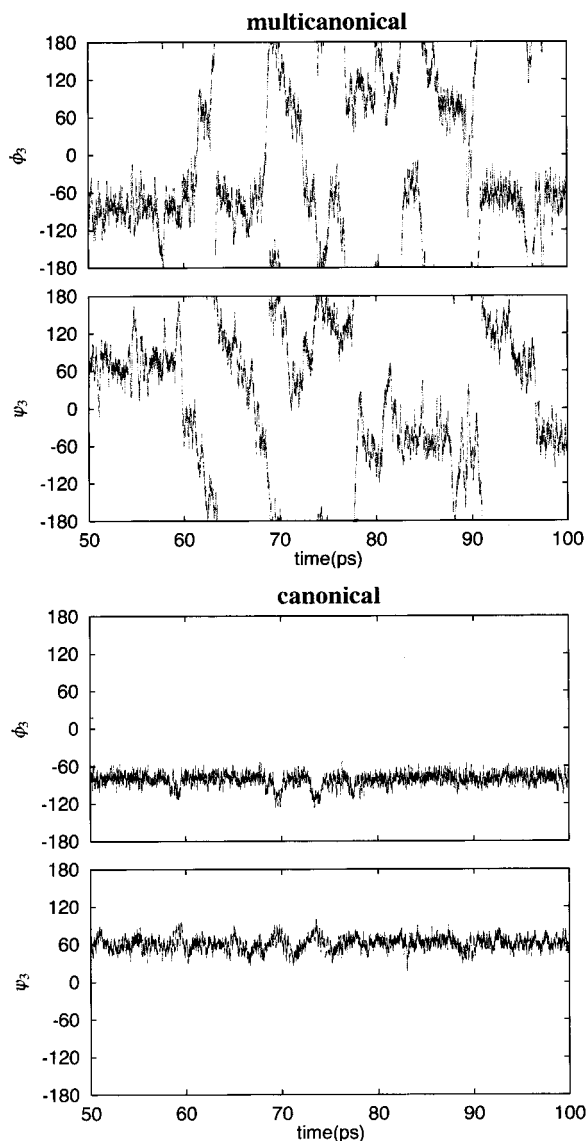


Figure 7. Time series of ϕ and ψ of Gly3. The upper is those of the multicanonical MD, and the lower is of the canonical MD.

The sampling efficiency of the multicanonical MD can also be seen in Figure 7, which shows time series of ϕ and ψ of Gly3 during the simulations. The values of ϕ and ψ in the multicanonical MD run indicate that the deformed potential of the multicanonical MD, E_{mc} , is flat enough to make the trajectory almost a random flight in the ϕ – ψ space. On the other hand, in the canonical simulation, ϕ and ψ fluctuate within a small range corresponding to the single peak of Figure 5. Figure 8 shows some representative structures found in the multicanonical MD. They are extremely diverse in both the main-chain and the side-chain conformations. These figures demonstrate that the multicanonical MD is capable of sampling large conformational space.

Finally, the computational burden of multicanonical MD is mentioned. In principle, CPU time of a simulation is proportional to the area under the curve of frequency of occurrence plotted against E . Hence, Figure 4 indicates that the multicanonical simulation sampling a wide range of the potential energy requires much more CPU time than the conventional canonical simulation. However, as shown clearly in Figures 5–7, even after the same CPU time, the canonical simulation is confined in much smaller conformational space than the multicanonical simulation.

3.3. Dynamical Properties and Temperature Control in Multicanonical MD. In the previous section, we discussed the properties in the configuration space. Here, some characteristics in the momentum space are discussed briefly.

In the potential scaling multicanonical MD, the force \mathbf{f}_i^{mc} acting on atom i is given by eq 26. This equation indicates that \mathbf{f}_i^{mc} is obtained by scaling the force in the canonical MD, $\mathbf{f}_i = -\partial E/\partial \mathbf{q}_i$, with the factor dE_{mc}/dE as

$$\mathbf{f}_i^{mc} = \frac{dE_{mc}}{dE} \mathbf{f}_i \quad (30)$$

This leads us to find that the frequency of a vibrational mode in the multicanonical MD, ω_{mc} , is approximated by

$$\omega_{mc}^2 \cong \frac{dE_{mc}}{dE} \omega_c^2 \quad (31)$$

where ω_c is the frequency of the same vibrational mode in the canonical MD. From eq 7 and a form of the function $\ln P_c(E, T_0)$ (refer to Figures 2 and 4), the factor dE_{mc}/dE is a monotone decreasing function of E such that

$$\frac{dE_{mc}(E)}{dE} = 1 + kT_0 \frac{d \ln P_c(E, T_0)}{dE} > 1 \quad \text{for } E < \langle E \rangle \quad (32)$$

$$< 1 \quad \text{for } E > \langle E \rangle \quad (33)$$

where $\langle E \rangle$ is the average energy of the preliminary canonical ensemble. This implies that at low energy regions ($E < \langle E \rangle$) the system fluctuates more rapidly than the canonical system, and at high energy regions ($E > \langle E \rangle$) the fluctuations become slower than those of the canonical ensemble. In other words, the frequency ω_{mc} has a time dependence in accordance with the time dependence of E . This is a characteristic of trajectories in the momentum space when the potential scaling multicanonical MD is performed.

Such dynamical properties cause difficulties in the temperature control by the Nosé–Hoover method. In the canonical MD by the Nosé–Hoover method, the fluctuation of the temperature is approximated by a harmonic oscillator, whose frequency ω_T is determined by a parameter Q , corresponding to the mass of the heat bath.^{23,33} To control the temperature adequately, we have to set ω_T close to the frequency of a typical vibration in the system by adjusting the parameter Q .²³ In the multicanonical MD, the typical frequency has time dependence, in contrast to that in the canonical MD. Thus, it is difficult to set up the simulation parameter Q for suitable temperature control. Since the constraint method does not have this problem, it is concluded that the constraint method, not the Nosé–Hoover method, should be used as the thermostat in the potential scaling multicanonical MD.

4. Conclusions

We have proposed multicanonical MD, which is powerful enough to efficiently sample molecular conformations. The simple algorithm of the potential scaling method has been confirmed to generate the multicanonical ensemble, with the aid of the constraint method to control the temperature. In contrast, it was shown that the temperature scaling method does not generate the multicanonical ensemble. Structural sampling of a short peptide molecule was performed, and it was shown that the current method efficiently explored much larger conformational space than the conventional canonical MD. For

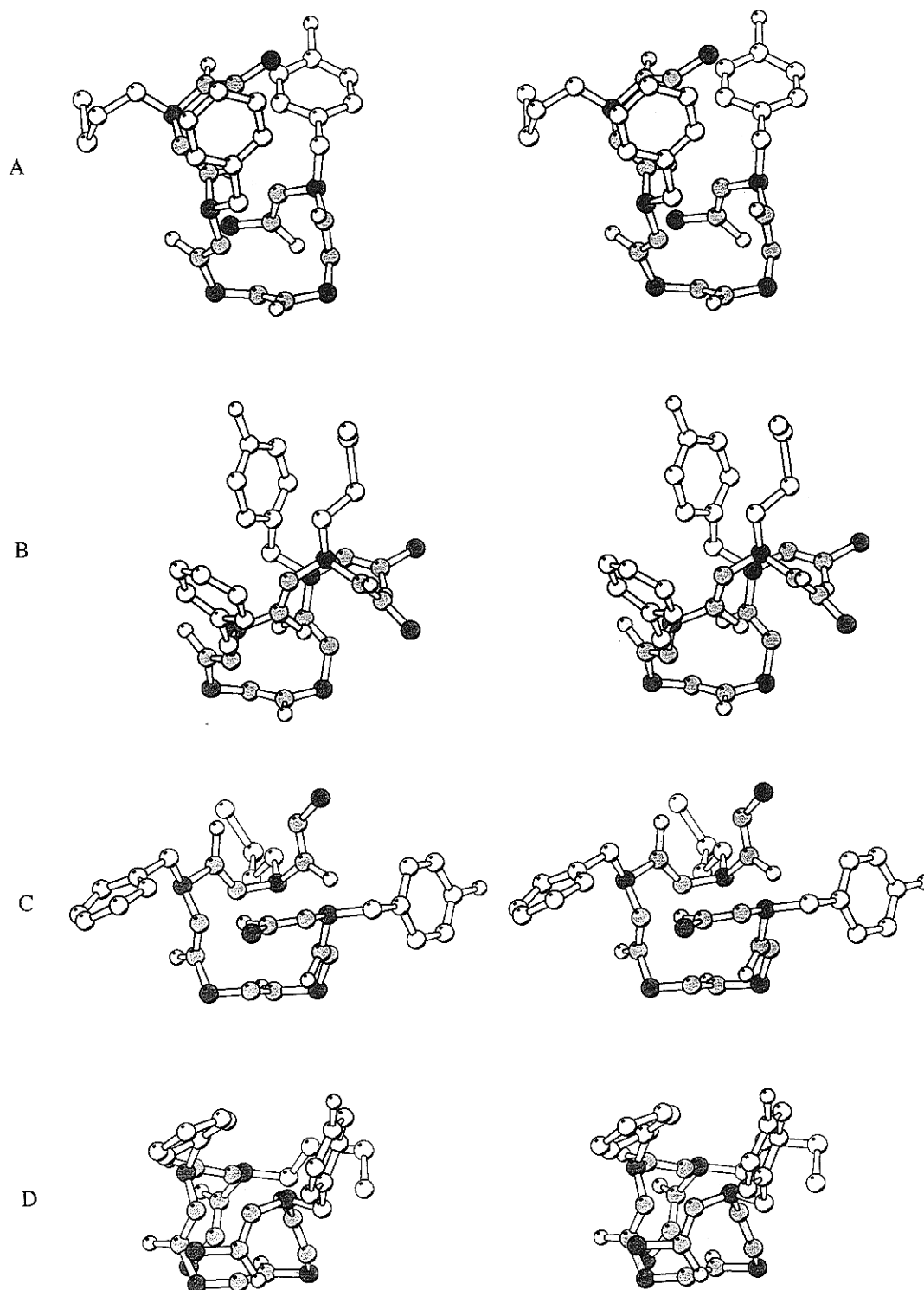


Figure 8. Stereoviews of some representative structures at 300 K of Met-enkephalin sampled by multicanonical MD. The structures A, B, C, and D are those included by the four groups shown in Figure 6: $(\phi_2, \psi_2, \phi_3, \psi_3) = (+, +, +, -), (-, +, +, -), (+, -, -, -), (-, -, -, -)$, respectively. The four structures were chosen randomly so that their energies are nearly equal to the average energy of the canonical ensemble at 300 K (≈ -115 kcal/mol). No hydrogen atoms are shown. This figure was drawn by the program MolScript.³⁴

complex chain molecules, such as a protein with solvent molecules, multicanonical MD will be the most powerful tool to find all the possible conformations at a given temperature. It is expected that this method will provide much more reliable structure models and predictions of biological macromolecules.

Acknowledgment. This study was inspired by a discussion with Dr. Y. Okamoto and Dr. U. H. E. Hansmann. We thank Dr. M. Saito for helpful discussions.

References and Notes

- (1) Berg, B. A.; Neuhaus, T. *Phys. Lett.* **1991**, B267, 249.
- (2) Berg, B. A.; Neuhaus, T. *Phys. Rev. Lett.* **1992**, 68, 9.
- (3) Berg, B. A.; Celik, T. *Phys. Rev. Lett.* **1992**, 69, 2292.
- (4) Lee, J. *Phys. Rev. Lett.* **1993**, 71, 211.
- (5) Berg, B. A.; Hansmann, U. H. E.; Okamoto, Y. *J. Phys. Chem.* **1995**, 99, 2236.
- (6) Hao, M.-H.; Scheraga, H. A. *J. Phys. Chem.* **1995**, 99, 2238.
- (7) Marinari, E.; Parisi, G. *Europhys. Lett.* **1992**, 19, 451.
- (8) Lee, J.; Choi, M. Y. *Phys. Rev.* **1994**, E50, R651.
- (9) Hesselbo, B.; Stinchcombe, R. B. *Phys. Rev. Lett.* **1995**, 74, 2151.

- (10) Hansmann, U. H. E.; Okamoto, Y. *J. Comput. Chem.* **1993**, *14*, 1333.
- (11) Hao, M.-H.; Scheraga, H. A. *J. Phys. Chem.* **1994**, *98*, 4940.
- (12) Okamoto, Y.; Hansmann, U. H. E. *J. Phys. Chem.* **1995**, *99*, 11276.
- (13) Kidera, A. *Proc. Natl. Acad. Sci. U.S.A.* **1995**, *92*, 9886.
- (14) Ferrenberg, A. M.; Swendsen, R. H. *Phys. Rev. Lett.* **1988**, *61*, 2635.
- (15) Metropolis, N.; Rosenbluth, A. W.; Rosenbluth, M. N.; Teller, A. H.; Teller, E. *J. Chem. Phys.* **1953**, *21*, 1087.
- (16) Northrup, S. H.; McCammon, J. A. *Biopolymers* **1980**, *19*, 1001.
- (17) Torrie, G. M.; Valleau, J. P. *Chem. Phys. Lett.* **1974**, *28*, 578.
- (18) Torrie, G. M.; Valleau, J. P. *J. Comput. Phys.* **1977**, *23*, 187.
- (19) Northrup, S. H.; Pear, M. R.; Lee, C.-Y.; McCammon, J. A.; Karplus, M. *Proc. Natl. Acad. Sci. U.S.A.* **1982**, *79*, 4035.
- (20) Hansmann, U. H. E.; Okamoto, Y. *Physica A* **1994**, *212*, 415.
- (21) Evans, D. J.; Morriss, G. P. *Phys. Lett.* **1983**, *98A*, 433.
- (22) Hoover, W. G. *Phys. Rev.* **1985**, *A31*, 1695.
- (23) Nosé, S. *Prog. Theor. Phys. Supp.* **1991**, *103*, 1.
- (24) Hoover, W. G.; Ladd, A. J. C.; Moran, B. *Phys. Rev. Lett.* **1982**, *48*, 1818.
- (25) Evans, D. J. *J. Chem. Phys.* **1983**, *78*, 3297.
- (26) Hockney, R. W. *Methods Comput. Phys.* **1970**, *9*, 136.
- (27) Brown, D.; Clarke, J. H. R. *Mol. Phys.* **1984**, *51*, 1243.
- (28) Martyna, G. J.; Klein, M. L.; Tuckerman, M. J. *J. Chem. Phys.* **1992**, *97*, 2635.
- (29) Morikami, K.; Nakai, T.; Kidera, A.; Saito, M.; Nakamura, H. *Comput. Chem.* **1992**, *16*, 243.
- (30) Weiner, S. J.; Kollman, P. A.; Nguyen, D. T.; Case, D. A. *J. Comput. Chem.* **1986**, *7*, 230.
- (31) Li, Z.; Scheraga, H. A. *Proc. Natl. Acad. Sci. U.S.A.* **1987**, *84*, 6611.
- (32) Némethy, G.; Pottle, M. S.; Scheraga, H. A. *J. Phys. Chem.* **1983**, *87*, 1883.
- (33) Nosé, S. *Mol. Phys.* **1984**, *52*, 255.
- (34) Kraluis, P. J. *J. Appl. Crystallogr.* **1991**, *24*, 946.